$Mg_3V_2O_8$: A Promising Cathode Material for Aqueous Mg-ion Battery

Xiu-Fen Ma, Hong-Yi Li, Daibo Gao, Weiwei Ren, Jiang Diao, Bing Xie,
Guangsheng Huang, Jingfeng Wang, and Fushang Pan

Abstract

The aqueous Mg-ion batteries (RMBs) have attracted lots of attention due to the high safety characteristics, low cost, and similar electrochemical characteristics to lithium. Magnesium orthovanadate ($Mg_3V_2O_8$, MVO) has stable three-dimensional framework and large ion channels and is expected to be a high-performance energy storage electrode material. Herein, low-cost $Mg_3V_2O_8$ cathode for RMBs is prepared by high-temperature calcination with the aqueous Mg^{2+} electrolyte. As a result, the MVO not only exhibits excellent electrochemical rate capability (the reversible discharge specific capacity is 143 mAh g^{-1} at the current density of 0.05 A g^{-1}, and it still remains 61 mAh g^{-1} at a large current density of 4 A g^{-1}), but also expresses good cycling performance (81% capacity retention after 10,000 cycles at the current density of 3 A g^{-1}). This work proves that the MVO is an exceptional candidate for MIBs.

Keywords

Magnesium orthovanadate • Aqueous Mg-ion battery • Cathode materials • Energy storage

Introduction

With the rapid consumption of nonrenewable fossil fuels over the past decades, growing concerns on environmental issues and energy crisis [1, 2]. In order to achieve sustainable development, clean energy utilization, such as solar energy and wind energy and tidal energy, has become an urgent task of human society [3]. The exploitation of electric vehicles and smart grids is the general trend of world development. High-performance secondary batteries as the energy storage system play a key role in electric vehicles and smart grids [4]. At present, lithium-ion batteries (LIBs) as one of the most popular energy storage devices have been widely applied to portable electronics owing to its high energy density, long cycling stability, and mature market [5, 6]. However, the safety problems, limited lithium resource, and increased prices still hinder the further development of LIBs [7]. Therefore, there is an urgent need for alternative energy with abundant resources and low cost to tackle the above problems. Aqueous magnesium-ion batteries (AMIBs), an ideal substitute for LIBs, have a great potential for the large-scale energy storage applications because of its earth-abundant storage, high security, low price, low reduction potential of Mg metal (−2.4 V vs. SHE), and high theoretical volumetric capacity (3833 mAh cm^{-3} for Mg vs. 2046 mAh cm^{-3} for Li) [8]. Also, compared with organic electrolyte, aqueous electrolyte can greatly improve the ionic conductivity of salt and has the advantages of low cost, non-toxic, non-flammable, and low requirements for production environment [9–11]. Nevertheless, the divalent magnesium ions carry twice as much charge as the monovalent lithium ions while the ionic radius of magnesium (0.72 Å) is similar to lithium (0.76 Å), which causes strong polarization effect and sluggish diffusion kinetics of Mg^{2+} in host materials, resulting in unsatisfactory energy and power densities [12, 13]. Thus, one of the most crucial tasks in RMBs is searching for ideal cathode materials.

Vanadate is an important vanadium-based material. Compared with vanadium oxide, vanadate has more stable crystal structure, better cycle stability, and longer cycle life. This is because the metal cation has a high energy barrier, which is not easy to leave the lattice node position during charge and discharging process. It plays a role in supporting

---

X.-F. Ma · H.-Y. Li (✉) · D. Gao · W. Ren · J. Diao · B. Xie · G. Huang · J. Wang · F. Pan
College of Materials Science and Engineering, Chongqing University, Chongqing, 400044, China
e-mail: hongyi.li@cqu.edu.cn

H.-Y. Li · J. Diao · G. Huang · J. Wang · F. Pan
National Engineering Research Center for Magnesium Alloys, Chongqing University, Chongqing, 400044, China

© The Minerals, Metals & Materials Society 2023

S. Barela et al. (eds.), *Magnesium Technology 2023*, The Minerals, Metals & Materials Series,
https://doi.org/10.1007/978-3-031-22645-8_39

and stabilizing the crystal structure and is conducive to maintaining the cyclic stability of the electrode material [14, 15]. Simultaneously, vanadium has multiple chemical valence states (V^{3+}, V^{4+} and V^{5+}) and can be coordinated with oxygen to form various open V-O ligands. A variety of metal cations, such as alkali metal ions (Li^+, Na^+, K^+ and Rb^+), alkali earth metal ions (Ca^{2+}, Mg^{2+}, and Sr^{2+}), transition metal ions (Ag^+, Cu^{2+}, Zn^{2+}, Co^{2+}, etc.), and others (Al^{3+}, In^{3+}, Bi^{3+}, NH^{4+}, etc.) can be inserted into V-O polyhedron to directly composited with it, resulting vanadate display various electrochemical properties because of different components introduction [16–19]. Thus, vanadate has a broad application prospect in the field of energy storage.

In the present work, we report magnesium orthovanadate ($Mg_3V_2O_8$, MVO) prepared by a high temperature calcination method. MVO has a stable three-dimensional framework and large ion channels and is expected to become a high-performance energy storage electrode material. As expected, the corresponding results show that the MVO is an ideal cathode material. It displays an initial discharge capacity of 143 mAh g^{-1} and the average discharge voltage of $\sim$2.34 V (vs. Mg^{2+}/Mg) using 4.5 M $Mg(NO_3)_2$ in deionized water as the electrolyte. Even at a high current density of 4 A g^{-1}, a reversible capacity of 61 mAh g^{-1} is obtained. In addition, the MVO cathode material exhibits an excellent cycling stability (10,000 cycles, 81% capacity retention) at high current density (3 A g^{-1}).

Experiment

Synthesis of Samples

All reagents were analytically pure and without further purification. $Mg_3V_2O_8$ was prepared by a high-temperature calcination method, which was reported by Li et al. before [20]. For a typical synthesis experiment, the raw materials V_2O_5 and MgO were first sieved to a uniform particle size of 45–75 µm. Then, MgO and V_2O_5 were mixed in a ceramic crucible (O.D. 9 cm, H 3.5 cm) in a molar ratio of 3 and calcined in a muffle furnace at 1223 K for 12 h. Finally, the white MVO powder was obtained and was used for the microstructural and the electrochemical characterizations.

Characterization

The crystallographic information of the prepared sample was measured by X-ray diffractometer (XRD, X'Pert PRO MPD) with Cu Kα radiation (λ = 0.1514178 nm) in 2θ range of 10–90° at 0.02° s^{-1} scan rate. The X-ray photoelectron spectroscopy (XPS) analysis was performed using a Thermo ESCALAB 250XI spectrometer with a monochromatized Al Kα X-ray. The morphology and microstructure of product was measured by field transmission electron microscopy (FESEM, TESCAN MIRA4) and transmission electron microscopy (TEM, Talos F200S).

Electrochemical Measurements

The electrochemical properties were measured at room temperature using CR2432 coin cells assembled in atmospheric air, which was fabricated by MVO electrode as cathode, activated carbon (AC) electrode as anode, saturated magnesium nitrate (4.5 M $Mg(NO_3)_2$) as aqueous electrolyte, and a Whatman Glass microfiber filter (Grade GF/A) was used as the separator. For the preparation of the electrodes, a slurry composed of 80 wt% MVO, 10 wt% acetylene black and 10 wt% polyvinylidene fluoride (PVDF) dispersed in 1-methyl-2-pyrrolidone (NMP). The obtained electrodes were prepared by coating the slurry onto carbon fiber papers (diameter 12 mm) with a mass loading of active material about 1 mg cm^{-2}, then drying in vacuum at 80 °C for 12 h. The cyclic voltammetry (CV) and electrochemical impedance spectroscopy (EIS) are collected using a electrochemical workstation (CHI 660E, Chenhua). The impedance data were recorded within the frequency range of 0.01–10,000 Hz. The galvanostatic charge–discharge tests were measured in the potential range of −1.1–1.4 V versus AC (1.3–3.8 V vs. Mg^{2+}/Mg) at different current densities using a multichannel battery testing machine (CT4008A, Neware). The assembled coin cells were aged for several hours before the charging/discharging process to ensure that the electrodes can be completely wetted.

Results and Discussion

The X-ray diffraction (XRD) patterns is displayed in Fig. 1a to investigate the crystallographic structure of the as-prepared sample. All the diffraction peaks are consistent with $Mg_3V_2O_8$ (JCPDS No 73-0207) with lattice parameters of a = 6.053 Å, b = 11.442 Å, c = 8.33 Å, $\alpha = \beta = \gamma =$ 90.0°, indicating the successful synthesis of MVO powder without any impurities. Meanwhile, the sharp diffraction peaks at 2θ equal to 19.70, 27.11, 29.67, 31.24, 35.21, 35.92, 43.62 and 63.14, which correspond to the (111), (112), (131), (040), (132), (023), (240), and (244) planes, indicating good crystallinity of the obtained MVO. Figure 1b demonstrates crystal structure of the orthorhombic MVO, where [VO_4] tetrahedra and edge-shared [MgO_6] octahedra are linked to oxygen atoms at the vertices. It forms a stable three-dimensional framework and a large ion channel, which is very conducive to the insertion/desertion of metal ions. The X-ray photoelectron spectrum (XPS) was

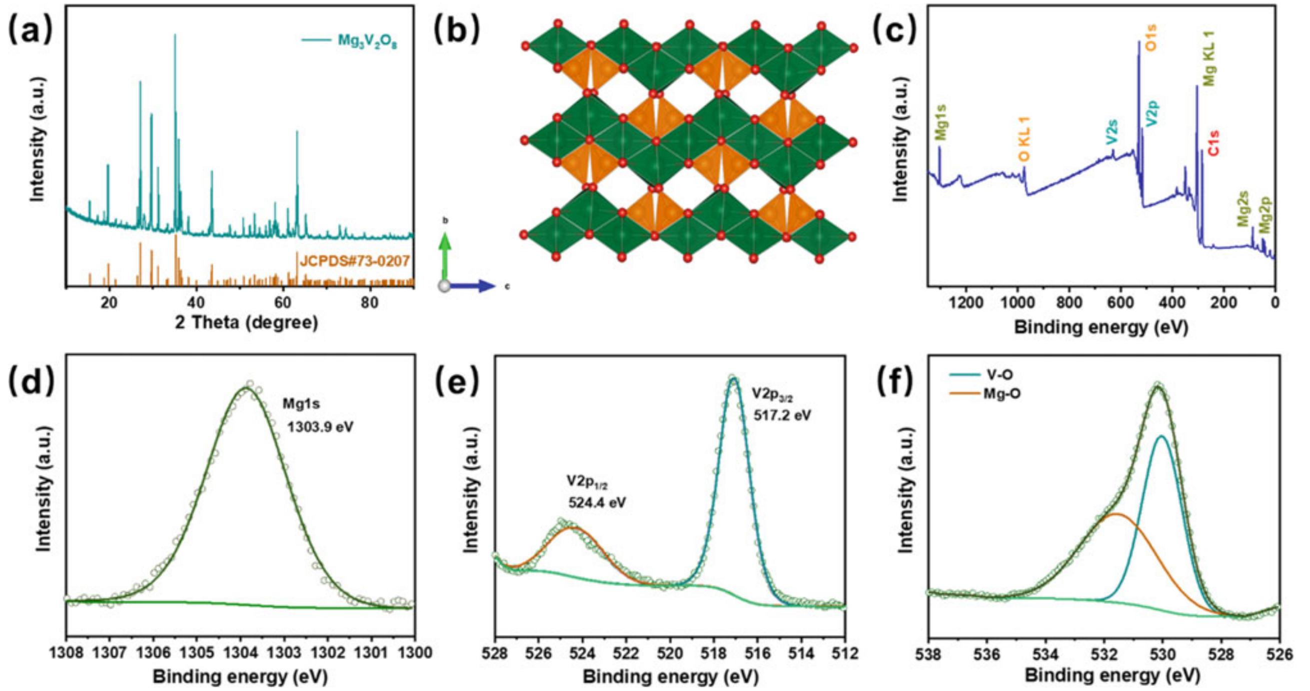

Fig. 1 XRD pattern of the MVO (**a**), crystal structure of MVO (**b**), XPS survey spectrum of MVO (**c**), XPS spectra of Mg 1s (**d**), V 2p (**e**), and O 1s (**f**) in MVO

used to further investigate the composition of the MVO. As is we can see in the survey spectrum (Fig. 1c), Mg, V, and O elements were detected. The Mg 1s, V 2p, and O 1s spectra was showed in Fig. 1d–f. The Mg 1s peak located at 1303.9 eV. In V 2p spectra, it shows two asymmetric peaks, which are related to V $2p_{1/2}$ (517.2 eV) and V $2p_{3/2}$ (524.4 eV) orbitals, belonging to V^{5+}. According to the O 1s core level, two distinct components at 530.1 eV and 533.2 eV correspond to V-O layers and Mg-O, respectively [21]. The morphology of the synthesized MVO is analyzed through SEM characterization, as shown in Fig. 2a–b, it is obvious that the products are irregular micron particles with size of 2–3 μm. According to energy dispersive X-ray spectroscopy (EDS) elemental mappings in Fig. 2c–f, the Mg, V and O atoms are homogeneously distributed in the MVO sample.

The magnesium storage electrochemical properties of MVO as cathode material were examined in the coin-type cells with 4.5 M $Mg(NO_3)_2$ as aqueous electrolyte, using the AC electrode as anode. Firstly, the typical cyclic voltammetry (CV) curves were measured at the scan rate of 0.1 mV s^{-1}, 0.2 mV s^{-1}, 0.3 mV s^{-1} and 0.4 mV s^{-1}, respectively, within the potential range from 1.1 to 3.8 V (vs. Mg^{2+}/Mg) (Fig. 3a). Three anodic peaks are observed around 1.8, 2.5 and 3.6 V, and three cathodic peaks are situated at 3.0, 2.3 and 1.5 V, which ascribed to the extraction and insertion potential of Mg^{2+}, respectively. The galvanostatic charge/discharge testing was used to further evaluated the electrochemical performance. As is shown in Fig. 3b, it exhibits the rate performance of the MVO at different current densities ranging from 0.05 to 4 A g^{-1}, delivering the reversible and stable capacities of 143, 108, 87, 82, 78, 76, 70, 65, and 61 mAh g^{-1}, respectively. When the current density returns to 0.05 A g^{-1}, the specific capacity retains 136 mAh g^{-1}, indicating outstanding structural stability of MVO electrode to withstand large-current tests, robust reaction kinetics and excellent rate capability. Figure 3c presents the corresponding galvanostatic charge–discharge curves of MVO at different current densities. As the current density increase, all these curves display similar voltage plateau behavior during charging and discharging process, a high average discharge voltage of ~2.34 V (vs. Mg^{2+}/Mg), relating to redox reactions responsible for insertion/extraction of Mg^{2+}. Meanwhile, the discharge specific capacity of cell decreased from 144 to 63 mAh g^{-1}, owing to the charge and discharge time is short at high current density, and the ion or electron transfer, oxidation–reduction reaction, etc., do not get enough time. In addition, high current density will lead to supersaturation or over consumption of protons in the electrolyte, and the internal resistance and ion resistance coefficient will increase. All these reasons will lead to the reduction of specific capacity at high current density. To further demonstrate the cycling stability of MVO for Mg^{2+} storage, long-term cycling performance was conduced at 3 A g^{-1}, as shown in Fig. 3d. After 10,000 cycles, an impressive 81%

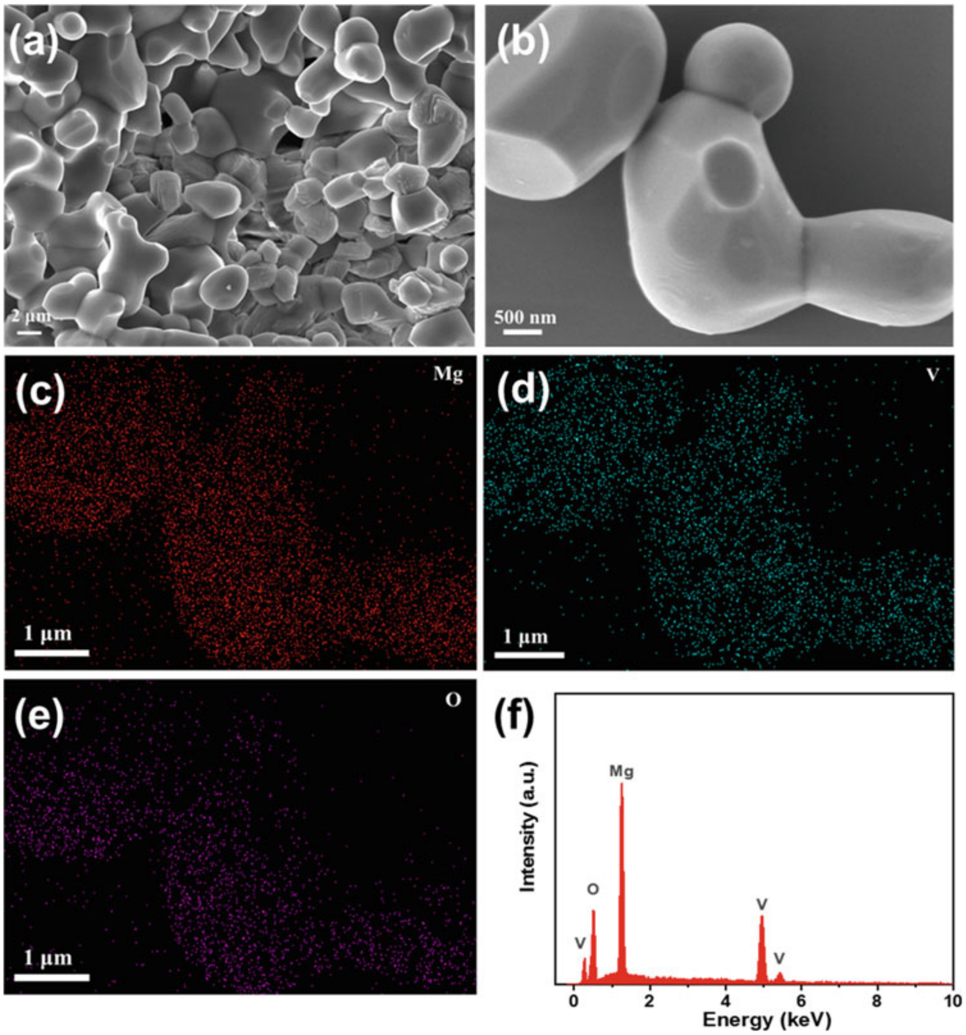

Fig. 2 SEM images of MVO (**a**–**b**), elemental mapping images of Mg (**c**), V (**d**), and O (**e**), energy dispersive X-ray (EDX) spectrum of the MVO (**f**)

retention of the initial capacity (68 mAh g^{-1}) indicates excellent structural stability, which may be attributed to the large three-dimensional ion channels in MVO. Concurrently, the high average Coulombic efficiency about 100% represents high reversibility of electrochemical Mg^{2+} storage and quantitative utilization of electrical charge. To study the ionic transportation kinetics, electrochemical impedance spectroscopy (EIS) experiments were employed. The intercept was corresponding to ohmic resistance (R_s) and the compressed semicircle in the high to medium frequency region was corresponding to charge transfer resistance (R_{ct}). An inclined line in the low-frequency range stands for the Warburg impedance (Z_W), which was related to the Mg^{2+} diffusion resistance in the active material. Among them, R_{ct} is the key factor that determines the charge and discharge rate performance. Zview software is used to establish the equivalent circuit model. As shown in Fig. 4a, the MVO electrode showed an ohmic resistance R_s of 4.38 Ω and charge transfer resistance R_{ct} of 3.72 Ω. The Mg^{2+} diffusion coefficient (D_{Mg}) could be calculated by Eqs. (1) and (2) to analyze the diffusion performance of Mg^{2+} in the electrode materials.

$$D_{Mg} = 0.5\left(RT/n^2F^2AC_{Mg}\sigma\right)^2 \tag{1}$$

$$Z' = R_s + R_{ct} + \sigma\omega^{-1/2} \tag{2}$$

where R is the gas constant, T is the absolute temperature, n is the number of the electrons per molecule attending the electronic transfer reaction, F is the Faraday constant, A is the surface area of the electrode, C_{Mg} is the concentration of magnesium ions, σ is the slope of the Z' versus $\omega^{1/2}$, which can be obtained from the line of $Z' \sim \omega^{1/2}$ (shown in Fig. 4b). The diffusion coefficients of Mg^{2+} was calculated by EIS method is about 9.15×10^{-13} cm s^{-2}. The small charge transfer impedance and the fast magnesium ion diffusion devoted to the preferable electrochemical rate performance.

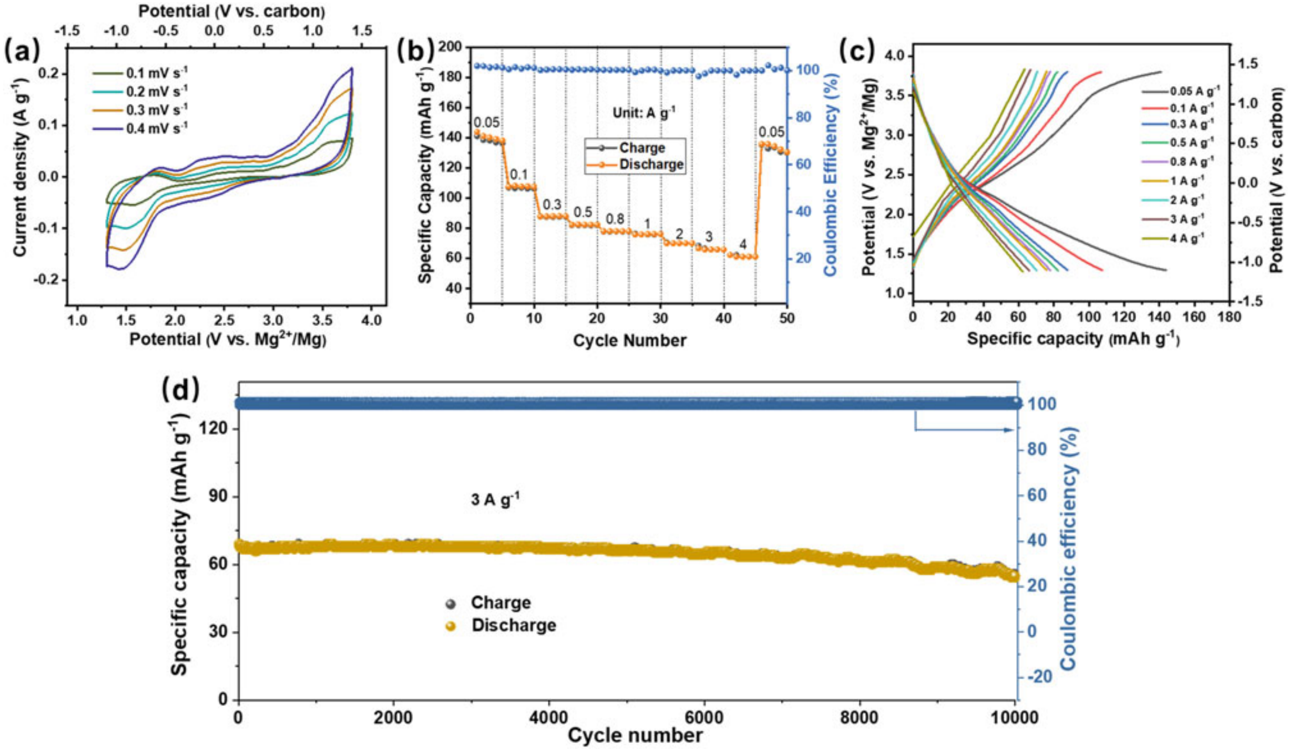

Fig. 3 CV curves of MVO at different sweep rates (**a**), rate performance (**b**), charge–discharge curves of MVO at different rates (**c**), cyclic performance of MVO at a current density of 3 A g^{-1} (**d**)

Fig. 4 Impedance spectra of the MVO electrode (**a**) and slope of the plots of Z' against $\omega^{-1/2}$ (**b**)

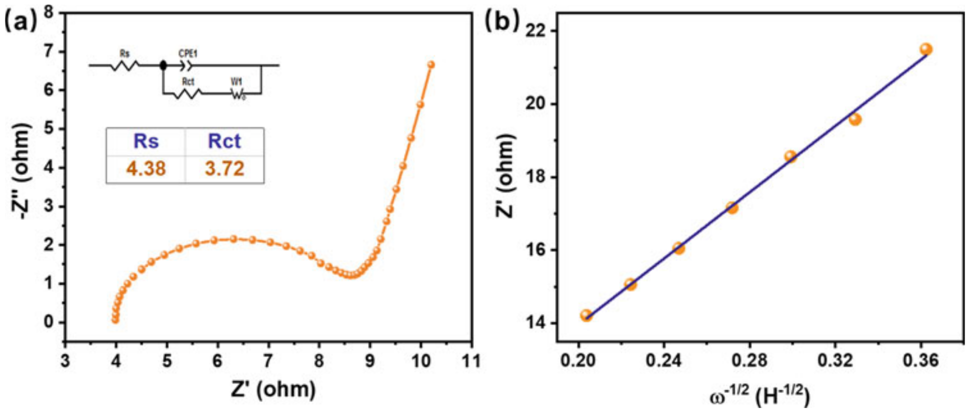

Conclusions

IN summary, the excellent electrochemical performance of MVO for magnesium-based battery are reported. The MVO as a cathode material exhibits initial specific capacity of 143 mAh g^{-1} at 0.05 A g^{-1} with a high average discharge voltage about 2.34 V (vs. Mg^{2+}/Mg) and shows remarkable long-term cyclic stability (81% capacity retention after 10,000 cycles at the current density of 3 A g^{-1}). It is worth noted that the MVO electrode delivers an impressive rate capacity, and the discharge capacities of MVO are 143, 108, 87, 82, 78, 76, 70, 65, and 61 mAh g^{-1} at 0.05, 0.1, 0.3, 0.5, 0.8, 1, 2, 3, and 4 A g^{-1}, respectively. When the current density returns to 0.05 A g^{-1}, the specific capacity is around 136 mAh g^{-1}, indicating outstanding structural stability of MVO electrode. This study demonstrates that MVO is a promising cathode material for magnesium ions storage, the excellent electrochemical performance can be attributed to its structure of stable three-dimensional framework and large ion channels.

Acknowledgements The authors would like to acknowledge the financial support by the National Natural Science Foundation of China (grant no. 52074050, 52222407), Chongqing Science and Technology Bureau (cstc2019jcyjjqX0006 and cstc2021ycjh-bgzxm0075).

References

1. H. Tang, C. Zuo, F. Xiong, C. Pei, S. Tan, P. Luo, W. Yang, Q. An, L. Mai, Flexible three-dimensional-networked iron vanadate nanosheet arrays/carbon cloths as high-performance cathodes for magnesium ion batteries, Sci. China Mater, 65 (2022): 2197–2206.
2. M. Karlsmo, R. Bouchal, P. Johansson, High-Performant All-Organic Aqueous Sodium-Ion Batteries Enabled by PTCDA Electrodes and a Hybrid Na/Mg Electrolyte, Angew Chem Int Ed Engl, 60 (2021): 24709–24715.
3. P. He, G. Zhang, X. Liao, M. Yan, X. Xu, Q. An, J. Liu, L. Mai, Sodium Ion Stabilized Vanadium Oxide Nanowire Cathode for High-Performance Zinc-Ion Batteries, Adv. Energy Mater, 8 (2018): e1702463.
4. H. Huang, D. Kundu, R. Yan, E. Tervoort, X. Chen, L. Pan, M. Oschatz, M. Antonietti, M. Niederberger, Fast Na-Ion Intercalation in Zinc Vanadate for High-Performance Na-Ion Hybrid Capacitor, Adv. Energy Mater, 8 (2018): e1802800.
5. Y. Liu, G. He, H. Jiang, I.P. Parkin, P.R. Shearing, D.J.L. Brett, Cathode Design for Aqueous Rechargeable Multivalent Ion Batteries: Challenges and Opportunities, Adv. Funct. Mater, 31 (2021): e2010445.
6. P. Canepa, G. Sai Gautam, D.C. Hannah, R. Malik, M. Liu, K.G. Gallagher, K.A. Persson, G. Ceder, Odyssey of Multivalent Cathode Materials: Open Questions and Future Challenges, Chem Rev, 117 (2017): 4287–4341.
7. H. Chen, J. Huang, S. Tian, L. Liu, T. Qin, L. Song, Y. Liu, Y. Zhang, X. Wu, S. Lei, S. Peng, Interlayer Modification of Pseudocapacitive Vanadium Oxide and Zn(H2 O)n (2+) Migration Regulation for Ultrahigh Rate and Durable Aqueous Zinc-Ion Batteries, Adv Sci, 8 (2021): e2004924.
8. L. Zhou, Q. Liu, Z. Zhang, K. Zhang, F. Xiong, S. Tan, Q. An, Y. M. Kang, Z. Zhou, L. Mai, Interlayer-Spacing-Regulated VOPO4 Nanosheets with Fast Kinetics for High-Capacity and Durable Rechargeable Magnesium Batteries, Adv. Mater, 30 (2018): e1801984.
9. D. Yang, Y. Zhou, H. Geng, C. Liu, B. Lu, X. Rui, Q. Yan, Pathways towards high energy aqueous rechargeable batteries, Coordin Chem Rev, 424 (2020): e213521.
10. F. Wang, X. Fan, T. Gao, W. Sun, Z. Ma, C. Yang, F. Han, K. Xu, C. Wang, High-Voltage Aqueous Magnesium Ion Batteries, ACS Cent Sci, 3 (2017): 1121–1128.
11. Y. Tang, X. Li, H. Lv, W. Wang, Q. Yang, C. Zhi, H. Li, High-Energy Aqueous Magnesium Hybrid Full Batteries Enabled by Carrier-Hosting Potential Compensation, Angew Chem Int Ed Engl, 60 (2021): 5443–5452.
12. Y. Liang, H.D. Yoo, Y. Li, J. Shuai, H.A. Calderon, F.C. Robles Hernandez, L.C. Grabow, Y. Yao, Interlayer-expanded molybdenum disulfide nanocomposites for electrochemical magnesium storage, Nano Lett, 15 (2015): 2194–2202.
13. X. Wang, X. Zhang, G. Zhao, H. Hong, Z. Tang, X. Xu, H. Li, C. Zhi, C. Han, Ether-Water Hybrid Electrolyte Contributing to Excellent Mg Ion Storage in Layered Sodium Vanadate, ACS Nano, 16 (2022): 6093−6102.
14. Q. An, Y. Li, H. Deog Yoo, S. Chen, Q. Ru, L. Mai, Y. Yao, Graphene decorated vanadium oxide nanowire aerogel for long-cycle-life magnesium battery cathodes, Nano Energy, 18 (2015): 265–272.
15. X. Wang, S. Zheng, S. Wang, Y. Zhang, H. Du, Self-anchoring dendritic ternary vanadate compound on graphene nanoflake as high-performance conversion-type anode for lithium ion batteries, Nano Energy, 22 (2016): 179–188.
16. H. Tang, Z. Peng, L. Wu, F. Xiong, C. Pei, Q. An, L. Mai, Vanadium-Based Cathode Materials for Rechargeable Multivalent Batteries: Challenges and Opportunities, Electrochem. Energy Rev, 1 (2018): 169–199.
17. M. Chen, Q. Liu, Z. Hu, Y. Zhang, G. Xing, Y. Tang, S.L. Chou, Designing Advanced Vanadium-Based Materials to Achieve Electrochemically Active Multielectron Reactions in Sodium/Potassium-Ion Batteries, Adv. Energy Mater, 10 (2020): e2002244.
18. S. Liu, L. Kang, J.M. Kim, Y.T. Chun, J. Zhang, S.C. Jun, Recent Advances in Vanadium-Based Aqueous Rechargeable Zinc-Ion Batteries, Adv. Energy Mater, 10 (2020): e2000477.
19. X. Xu, F. Xiong, J. Meng, X. Wang, C. Niu, Q. An, L. Mai, Vanadium-Based Nanomaterials: A Promising Family for Emerging Metal-Ion Batteries, Adv. Funct. Mater, 30 (2020): e1904398.
20. J. Cheng, C.-J. Wang, S. Shen, J. Diao, B. Xie, H.-Y. Li, Synthesis and Solubility Behavior of Magnesium Ortho-, Meta-, and Pyrovanadates, Jom, 74 (2021): 23–29.
21. Y. Zhu, G. Huang, J. Yin, Y. Lei, A.H. Emwas, X. Yu, O.F. Mohammed, H.N. Alshareef, Hydrated MgxV5O12 Cathode with Improved Mg2+Storage Performance, Adv. Energy Mater, 10 (2020): e2002128.